ACS APPLIED MATERIALS & INTERFACES

Research Article

www.acsami.org

Split-Second Nanostructure Control of a Polymer:Fullerene Photoactive Layer using Intensely Pulsed White Light for Highly Efficient Production of Polymer Solar Cells

Hee Yeon Yang,[†,‡] Jae-Min Hong,[†] Tae Whan Kim,[‡] Yong-Won Song,[†] Won Kook Choi,[†] and Jung Ah Lim*[,†]

[†]Interface Control Research Center, Future Convergence Research Division, Korea Institute of Science and Technology (KIST), Seoul 136-791, Korea

[‡]Department of Electronics and Computer Engineering, Hanyang University, Seoul 133-791, Korea

Supporting Information

ABSTRACT: Intensely pulsed white light (IPWL) treatment was tested as an ultrafast, large-area processable optical technique for the control of the nanostructure of a polymeric bulk-heterojunction photoactive layer to improve the efficiencies of polymer solar cells. Only 2 s of IPWL irradiation of a polymer:fullerene photoactive layer under ambient conditions was found to enhance significantly the power conversion efficiencies of the tested polymer solar cells to values approaching that of typical devices treated with thermal annealing. Consecutive white-light pulses from the xenon lamp induce the self-organization of the polymeric donor into an ordered structure and result in the optimized phase segregation of the polymeric donor and the fullerene acceptor in the photoactive layer, which enhances the light absorption and hole mobility and results in efficient photocurrent generation. The effects of varying the pulse conditions on device performance, including the irradiation fluence, pulse duration time, and number of pulses, were systematically investigated. Finally, it was successfully demonstrated that the IPWL treatment produces flexible polymer solar cells. The proposed IPWL process is suitable for the efficient industrial roll-to-roll production of polymer solar cells.

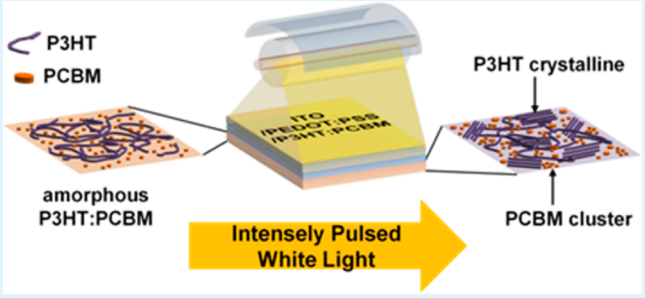

KEYWORDS: *intensely pulsed white light, polymer solar cells, nanostructure, self-organization*

1. INTRODUCTION

Polymer solar cells (PSCs) are light in weight and have low fabrication costs, high mechanical flexibility, and fast roll-to-roll (R2R) coating, and as a result have attracted attention as a promising renewable energy source.[1−7] Extensive efforts over the past decade have been devoted to improving their low efficiencies; a significant breakthrough was the introduction of the bulk-heterojunction (BHJ) structure, which consist of a blend of a polymeric electron donor (D) and a fullerene electron acceptor (A).[8] BHJ structures implement an ingenious solution to the limitations of PSCs (e.g., their large exciton binding energies[9] and small exciton diffusion lengths (5−10 nm)).[10,11] In a BHJ structure, the D−A interface area where excitons dissociate is much larger than in inorganic bilayer cells, and the photogenerated charge carriers travel to the electrodes through a bicontinuous interpenetrated network of D−A. However, many research groups have demonstrated that the power conversion efficiencies (PCEs) of BHJ-based PSCs are directly dictated by the nanostructure and morphology of their BHJ photoactive layers.[12,13]

To date, thermal annealing and solvent annealing (including slow solvent-drying methods) have been widely used as post-treatments to control the nanostructure of BHJ photoactive layers.[14−18] For example, in the case of PSCs based on poly(3-hexylthiophene) (P3HT):[6,6]-phenyl-C61-butyric acid methyl ester (PCBM), it is well-known that annealing the P3HT:PCBM photoactive layer is a key step to control the D−A phase-separation morphology and to improve the light absorption and charge-carrier mobility in the layer by inducing the self-organization of the polymeric electron donor. This approach is also beneficial for other photoactive materials, such as poly{2,6-(4,4-bis[2-ethylhexyl]-4*H*-cyclopenta[2,1-*b*;3,4-*b*0]-dithiophene)-alt-4,7-(2,1,3-benzothiadiazole)} (PCPDTTBT)[19] and poly(9,9′-dioctylfluorene-*co*-bithiophene) (F8T2)[20] thin films, for which thermal annealing leads to improved device performance by enhancing the polymer-chain stacking and the D−A phase-separation morphology.[19,20] Although such post-treatment methods are conventionally implemented in laboratory research, they are time-consuming, and the use of thermal ovens or solvent vapors is obviously

Received: September 13, 2013
Accepted: December 30, 2013
Published: December 30, 2013

 © 2013 American Chemical Society

problematic for the R2R production of PSCs. Although the PCEs are still low for practical energy needs, state-of-the-art PSCs have been closer to fast production using R2R methods. (Comprehensive review articles on R2R-based fabrication of PSCs are available.[6,7]) Recently, optical techniques such as microwave irradiation and pulsed-laser annealing have successfully been used as post-treatment methods for PSCs.[21−24] These optical approaches offer rapid, clean, and scalable methods for improving the efficiency of PSCs fabricated in industrial R2R production.

In this study, we tested a split-second large-area process using intensely pulsed white light (IPWL) for the control of the nanostructure of a BHJ thin film. The proposed IPWL treatment has substantial advantages: (i) short processing times on the order of milliseconds, (ii) surface-selectivity that does not damage flexible substrates, and (iii) no requirement for an inert-gas atmosphere.[25−36] IPWL basically consists of a xenon flash light like that of a camera flash. Recently, IPWL irradiation has been successfully demonstrated as a photoactive sintering process in printable nanoink sintering,[25−32] in the fabrication of $Cu(In_{1-x}Ga_x)Se_2$ (CIGS) thin films,[33,34] and in the nanogranulation of carbon nanotubes (CNTs) with metal-alloy nanoparticles.[35] For conjugated polymers, Huang et al. reported that under flash irradiation polyaniline nanofibres melt to form a smooth and continuous film from an originally random network of nanofibers.[37] Krebs group also reported that irradiation of highly intensive visible light[38] or xenon flash lamp[36] were explored as a method for selectively heating and transforming thermocleavable conjugated polymers such as poly[3-(2-methylhex-2-yl)oxycarbonlydithiophene] (P3MHOCT) or copolymers based on dithienylthiazolo[5,4-*d*]thiazole (DTZ) and silolodithiophene (SDT), which was used as a photoactive layer for large-area PSC modules. These studies have primarily focused on photothermal induced chemical reactions in the materials.

Here, we report our testing of IPWL irradiation as an optical-annealing method by which the nanostructure of the P3HT:PCBM photoactive layer is reconstructed to improve the device performance in a short period. An IPWL irradiation of P3HT:PCBM blend films of only 2.2 s was found to enhance significantly the PCEs of the devices and to produce efficiencies close to those of typical devices treated with thermal annealing. Our film-characterization results show that the performance enhancement resulting from the IPWL treatment arises from the self-organization of P3HT into an ordered structure and the phase segregation of P3HT and PCBM. The optimum pulse conditions were investigated by varying the irradiation fluence, pulse duration time, and number of pulses. The proposed IPWL process was successfully applied to flexible PSCs, which suggests that this process could be used in the R2R production of flexible PSCs.

2. EXPERIMENTAL SECTION

2.1. Device Fabrication. An ITO-patterned glass substrate was cleaned by performing sonication with acetone and isopropyl alcohol. Poly(3,4-ethylenedioxythiophene):poly(styrenesulfonic acid) (PEDOT:PSS) (Baytron P) was spin-coated onto the ITO glass substrate. After drying the PEDOT:PSS film at 100 °C for 30 min in a nitrogen-filled glovebox, the active layer of the P3HT (Reike Metal Inc.) and PCBM (Nano-C) blend film (1:0.83 weight ratio) was deposited by spin-coating from a blend solution in chlorobenzene at 2000 rpm for 40 s. The device was irradiated with IPWL through the ITO glass placed underneath the xenon flash lamp at a distance of 2 mm under ambient conditions. The active layer of the reference device was annealed at 150 °C for 10 min by using a hot plate under ambient conditions. Finally, LiF/Al electrodes with thicknesses of 0.6 nm/100 nm were thermally deposited through a shadow mask at a system pressure of ~10^{-6} Torr. The active area of the device was 4 mm^2. The flexible solar cell was constructed on a 2.5 × 2.5 cm^2 ITO/PET substrate using the same procedure as the glass substrate, and the active area of the unit device was 3 × 6 mm^2.

2.2. Intensely Pulsed White Light System. A homemade IPWL system was equipped with a xenon flash lamp (PerkinElmer QXF, UK), power supply, capacitors, and water-cooling system. The lamp head was chilled with water to maintain stable operation, and the position of the lamp was adjusted with a *z*-axis translation stage. The xenon flash lamp emitted a broad spectrum in the range of 400 to 1000 nm. The IPWL system was designed to provide up to 99 pulses on the millisecond scale with a minimum pulse duration of 0.1 ms. The energy of the light (irradiation fluence) was characterized by using a NOVA II laser power meter (OPHIR) and was varied by changing the number of pulses, pulse duration time, free temporal period, and voltage.

2.3. Characterization. The electrical properties of the devices were determined using a Keithley 2400 source-measure unit under ambient conditions. The photocurrent was obtained under illumination from a Thermal Oriel solar simulator (AM 1.5G, 100 mA/cm^2). We calibrated the light intensity using carefully calibrated silicon photovoltaic (PV) solar cells. The UV−vis absorption spectra of pristine, thermally treated, and IPWL-treated thin films were obtained with an Optizen 3220 UV−vis spectrometer. To investigate the molecular orientation of P3HT, X-ray diffraction (XRD) measurements were performed by using the 3D beamline at the Pohang Accelerator Laboratory, Korea. The wavelength of the X-ray source and the grazing incidence angle were 1.54 Å and 0.18°, respectively. Bright-field transmission electron microscopy (TEM) was performed under slightly defocusing conditions with a Technai F20 TEM operating at 200 kV. The P3HT:PCBM blend thin films were spin-coated onto PEDOT:PSS-coated ITO glass, immersed in deionized water, floated on the water surface, and then transferred to 200 mesh copper TEM grids. The changes in the chemical functional groups of P3HT exposed to pulsed white-light irradiation were investigated by analyzing the absorption spectrum obtained with a Fourier transform infrared spectrometer (FT-IR, Bruker IFS 66 V) using p-polarized light with an incidence angle of 80° under vacuum conditions. The surface morphologies of the P3HT:PCBM thin films were analyzed using atomic force microscopy (AFM) (XE-100) in noncontact mode.

3. RESULTS AND DISCUSSION

A schematic illustration of the IPWL treatment of a P3HT:PCBM film is shown in Figure 1a. The xenon flash lamp emits a broad spectrum of visible light in the range from 400 nm to 1 μm that covers the absorption of the P3HT:PCBM thin film (Figure 1b). IPWL is produced by using a pulse controller and a supercapacitor: the pulse controller triggers the supercapacitor, which delivers electrical current to the lamp within milliseconds. The consecutive light pulses are incident from the glass side. During IPWL irradiation, high-intensity light energy is delivered onto the sample within a few tens of milliseconds, which instantly increases the temperature of the sample because of the photothermal effect.[36−41] (Our detailed discussion of a possible mechanism of heat generation during IPWL treatment is presented later.) The fluence of the irradiation can be controlled by varying several properties of the pulse, such as the applied voltage, number of pulses, pulse duration time, and free temporal period (Figure 1c).

In Figure 2, the current density−voltage (*J*−*V*) characteristics of an IPWL-treated P3HT:PCBM BHJ solar cell are compared to those of a typical P3HT:PCBM device treated with a thermal-annealing process. The average photovoltaic

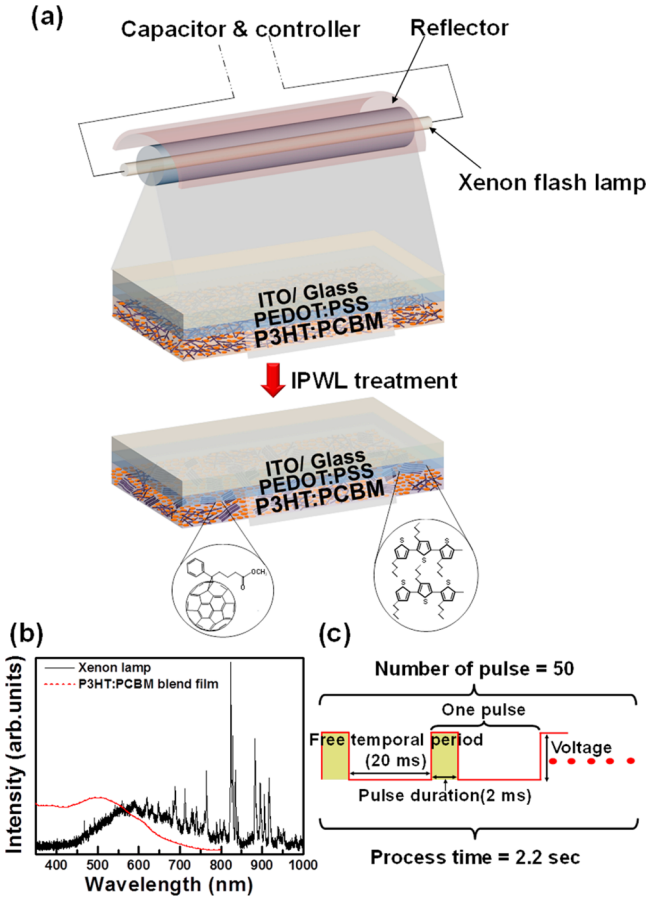

Figure 1. (a) Schematic of IPWL treatment for P3HT:PCBM blend films. (b) Spectra distribution of xenon flash lamp and P3HT:PCBM blend film. (c) Schematic for the pulse parameters of IPWL.

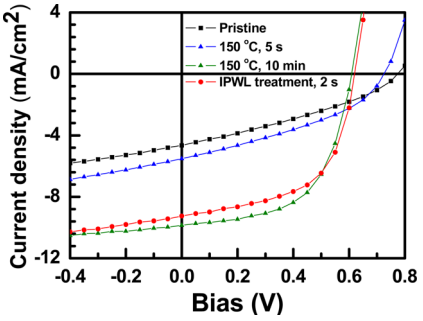

Figure 2. Current density–voltage (J–V) characteristics of polymer solar cells with pristine, thermal annealing at 150 °C for 5 s or 10 min, and IPWL treatment for 2 s.

performance parameters of the tested devices are summarized in Table 1. The thermal annealing of P3HT:PCBM at 150 °C for 10 min was found to improve the PCE of the device from 1.26 to 3.48%, which is close to commonly reported performances for P3HT:PCBM-based devices. Interestingly, the IPWL-treated device also exhibits an improved PCE of 3.27% with open circuit voltage (V_{oc}) = 0.62 V, short circuit current (J_{sc}) = −9.25 mA/cm^2, and fill factor (FF) = 0.57, which are close to the values for the typical device treated with thermal annealing. It should be noted that the total IPWL irradiation time was 2.2 s for a substrate area of 2.5 × 2.5 cm^2, which is short compared to the processing times of established post-treatment methods: thermal annealing (>5 min),[15] solvent annealing (>50 s),[18] microwave treatment (>90 s),[21] and pulsed-laser annealing (>4 s for device areas of 3 × 5 mm^2).[24] A video of the IPWL process is provided (Video S1, Supporting Information). As a comparison, thermal treatment for 5 s resulted in almost no improvement in device performance, as shown in Figure 2. Considering that the nanostructure of the P3HT:PCBM BHJ layer is the main factor determining device performance, this result suggests that the nanostructure of the P3HT:PCBM photoactive layer is reconstructed by a short period of IPWL irradiation.

The temperature of the substrate during the sequential deposition of the layers was directly monitored with a digital thermometer through a thermocouple attached to the substrate during the IPWL treatment. As shown in Figure 3a, as the irradiation fluence increases, the temperatures of the glass, ITO/glass, and PEDOT:PSS on ITO/glass layers increase gradually such that the substrates exhibited almost similar surface temperatures at each fluence. However, after the deposition of the P3HT:PCBM active layer, the temperature of the device dramatically increases. This result implies that photothermal conversion plays an important role in heat generation in the P3HT:PCBM layer during IPWL irradiation. In fact, 2.2 s IPWL irradiation with 50 pulses and a fluence of 35 J/cm^2 is sufficient to increase the device temperature to 108 °C, which is above the glass-transition temperature (T_g) of the P3HT:PCBM active layer (80 °C for 55:45 wt % of P3HT:PCBM).[42] The T_g determines the lower limit of the operating window for thermal annealing that is usually used to optimize BHJ morphologies. In contrast, thermal annealing using a hot plate needs at least 10 s to increase the temperature of the device to 100 °C, as shown in Figure 3b. In the photothermal effect, heat is generated by the absorption of light. In previous literature, photothermal conversion is observed for nanostructured materials such as single-walled carbon nanotubes (SWNTs), silicon nanowires, graphene nanosheets, and conjugated polymer, especially when they are exposed to a strong, pulsed-light source such as a camera flash.[36−41] The heat generated by flash irradiation can result in temperatures sufficiently high to ignite and reconstruct SWNTs and burn silicon nanowires, which require temperatures above ∼1500 °C. In this work, photothermal conversion in the P3HT:PCBM active layer can generate heat directly inside the P3HT:PCBM active layer. Additionally, because the conjugated polymer materials such as polyaniline have a low thermal conductivity,[43,44] the heat from photothermal conversion could

Table 1. Device Performance under Various Annealing-Treatment Conditions

condition	V_{oc} (V)	J_{sc} (mA/cm^2)	FF	PCE (%)
pristine	0.76 ± 0.01	−4.74 ± 0.44	0.35 ± 0.02	1.26 ± 0.1
IPWL treatment (ambient conditions, 2 s)	0.62 ± 0.01	−9.25 ± 0.3	0.57 ± 0.01	3.27 ± 0.1
thermal treatment (ambient conditions, 150 °C for 5 s)	0.72 ± 0.01	−5.52 ± 0.41	0.38 ± 0.01	1.50 ± 0.1
thermal treatment (ambient conditions, 150 °C for 10 min)	0.61 ± 0.01	−9.86 ± 0.19	0.58 ± 0.02	3.48 ± 0.06

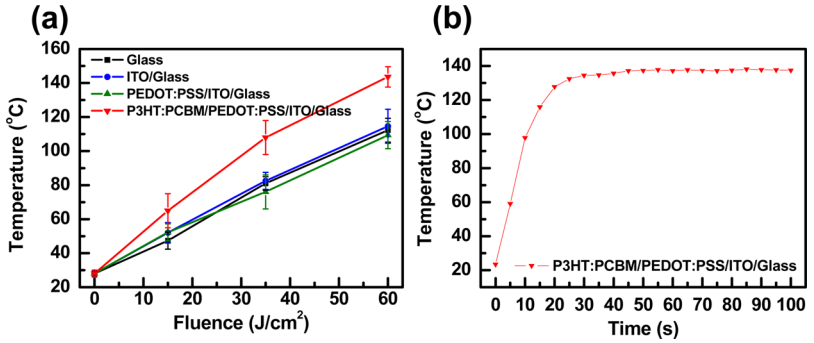

Figure 3. (a) Temperature of the substrates during the IPWL irradiation for various fluence conditions. (b) Temperature of the substrates during thermal annealing using a hot plate.

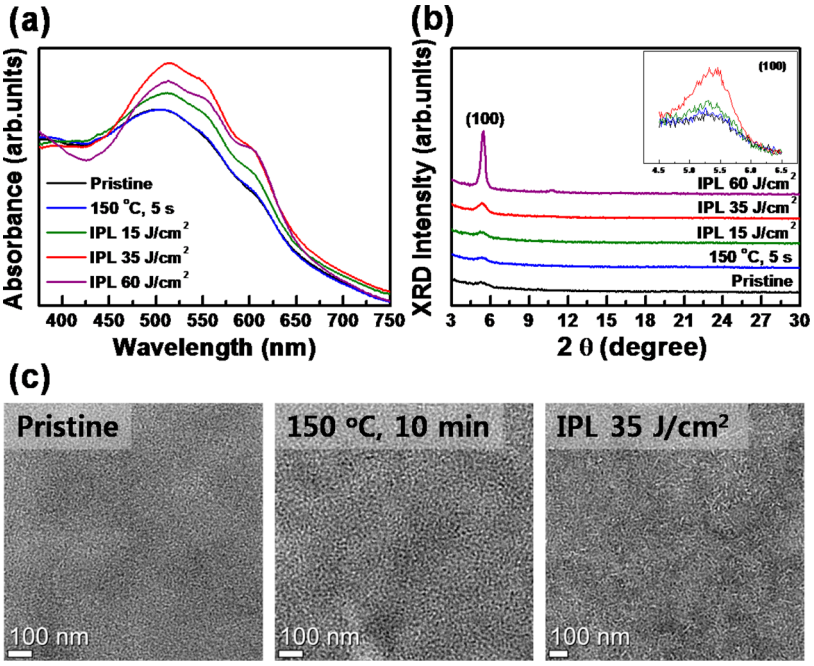

Figure 4. (a) UV−vis absorption and (b) out-of-plane-mode grazing incidence X-ray diffraction spectra of pristine and thermal-treated as well as various conditions of IPWL treatment. (c) Bright-field TEM image of P3HT:PCBM blend films under different annealing treatment conditions.

accumulate within the photoactive layer. By contrast, thermal annealing-based heat transfer requires sufficient time to transfer the heat from the hot plate to the P3HT:PCBM active layer passing through the glass, ITO, and PEDOT/PSS layers. Thus, the generation of heat by IPWL irradiation might be much faster than that achieved with thermal-annealing methods based on heat transfer.

Even though the heat-generation mechanism of flash irradiation is unclear, we believe that the absorption of light by P3HT:PCBM produces a temperature increase through nonradiative energy dissipation. The absorbance of the P3HT:PCBM thin films is 55.7% at wavelengths in the range of 350−800 nm, so P3HT:PCBM blend films can absorb nearly 14.4 J/cm^2 under IPWL exposure at a fluence of 35 J/cm^2. The melting energy of P3HT:PCBM (55:45 wt %) blend films can be calculated from the melting enthalpy determined with differential scanning calorimetry (DSC) (9.9 J/g for P3HT:PCBM = 55:45 wt % blend films (100 nm) with 10% crystallinity[45]) and was found to be approximately 1.27×10^{-4} J/cm^2. The photothermal conversion efficiency of P3HT:PCBM blend films is unknown, but if we assume that only 0.01% of the photoenergy absorbed from the incident beam is converted into heat, then more heat than is required for the melting of the P3HT:PCBM film is provided by the photothermal conversion of IPWL irradiation. In addition, previous reports on the relaxation dynamics of polymer crystallization indicate that polymer chains can crystallize on the time scale of milliseconds.[46,47] Yamamoto reported that polymer molecules crystallize into a neat chain folded lamella within several nanoseconds[39] and that the crystallinity initially increases by up to around 10% within 10 ns at any temperature.[47] Sasaki et al. also reported that the relaxation time required by polymer liquid crystals for a phase transition from nematic to isotropic is in the range of 10−100 ms.[48] Furthermore, it is known that PCBM and P3HT are highly miscible and that PCBM can penetrate into the P3HT layer through the P3HT amorphous region and form a BHJ structure within a few seconds of annealing.[49] These previous reports support the claim that the total process time of an IPWL treatment is sufficient to induce phase transitions in P3HT:PCBM blend films.

Figure 4a shows the UV−vis spectra of a pristine P3HT:PCBM blend film, of blend films after IPWL treatment under various fluence conditions, and of a blend film after

thermal treatment at 150 °C for 5 s. Thermal treatment at 150 °C for 5 s produces a similar spectrum to that of the pristine film. After IPWL treatment, absorption shoulders appear at 550 and 600 nm, which indicates that interchain ordering of P3HT has occurred, resulting in the formation of an extended conjugated system.[50] To investigate the changes in the chain orientation and crystallinity of the P3HT:PCBM blend films resulting from IPWL treatment under various fluence conditions, out-of-plane X-ray diffraction (XRD) was performed. Figure 4b shows that the intensity of the (100) peak, originating from the edge-on ordering of P3HT chains, increases with increases in the IPWL fluence. Because the hole mobility in P3HT is proportional to the crystallinity, which is related to the degree of $\pi-\pi$ P3HT-interchain stacking, this result implies that IPWL treatment improves the hole mobility of P3HT:PCBM films. We investigated the effects of the IPWL treatment on the morphology of the P3HT:PCBM blend films using atomic force microscopy (AFM). After IPWL treatment, the surface morphology of P3HT:PCBM film turned rough compared to the pristine film, and the RMS roughness of the P3HT:PCBM thin films increases from 0.58 to 1.1 nm (see Supporting Information Figure S4). In the previous literature, the surface morphology of P3HT:PCBM photoactive layers roughened with nanophase separation of P3HT:PCBM after thermal or solvent annealing.[51] To show tangible proof for the morphological development of the P3HT:PCBM thin films, transmission electron microscopy (TEM) analysis was performed for the pristine, thermally treated, and IPWL-treated P3HT:PCBM blend thin films, as shown in Figure 4c. The pristine film has a smooth, homogeneous morphology, whereas distinct rodlike P3HT crystals are present in the thermally and IPWL-treated films. In bright-field TEM imaging, P3HT crystals appear bright and PCBM regions appear dark because the density of P3HT crystals (1.10 g/cm^3) is lower than that of PCBM (1.50 g/cm^3).[52,53] On the basis of these results, we conclude that IPWL irradiation induces both the self-organization of P3HT into an ordered structure and the optimized phase segregation of P3HT and PCBM, which both enhance light absorption and hole mobility as well as efficient photocurrent generation.

Figure 5a shows the $J-V$ characteristics of photovoltaic devices annealed with IPWL under various fluence conditions. The statistical data for the performances of these devices are presented in Figure 5b. Below a threshold fluence of 15 J/cm^2, almost no change in J_{sc} and PCE is observed. Above this threshold, J_{sc} and PCE increase with increasing fluence until the maximum value is reached, after which J_{sc} and PCE start to decrease. For the optimum IPWL treatment fluence of 35 J/cm^2, J_{sc}, V_{oc}, FF, and PCE reach −8.31 mA/cm^2, 0.62 V, 0.58, and 3.0%, respectively. The decrease in V_{oc} can be explained by the change in the oxidation potential of the P3HT phase; an increase in the crystallinity of P3HT results in a lower oxidation potential.[54,55] Above 35 J/cm^2, the photovoltaic performance deteriorates. After irradiation at fluences of 50 and 60 J/cm^2, the devices exhibit low PCEs of 2.32 and 1.49% and low J_{sc} values of −6.45 and −5.22 mA/cm^2, respectively. These reductions in performance are due to the photodegradation and oxidation of P3HT. As shown in Figure 4a, the light absorbed by the P3HT:PCBM blend film treated with IPWL at 60 J/cm^2 is lower than those treated with weaker fluences. This decreased light absorption is due to a reduced conjugation length and disruption, which is related to photobleaching of the polymer.[56] Supporting Information Figure S2 shows photographs of a

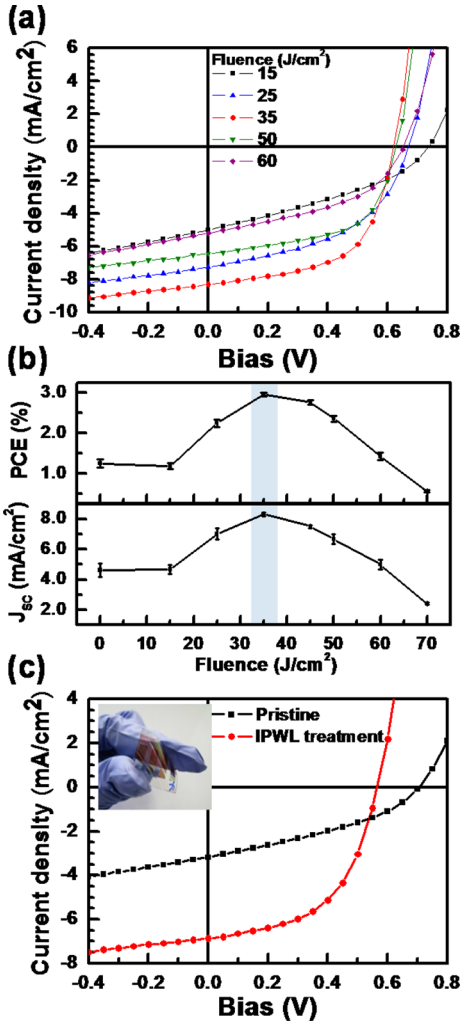

Figure 5. (a) $J-V$ characteristics and (b) J_{sc} and PCE variation of the devices annealed with IPWL under various fluence conditions. (c) $J-V$ characteristics of polymer solar cells on the flexible substrate for pristine and IPWL treatment.

pristine P3HT:PCBM blend film and blend films after IPWL treatment under various fluence conditions. The color of the P3HT:PCBM blend film treated with a IPWL fluence of 35 J/cm^2 has become deep violet in the IPWL treatment region, which is related to the appearance of the absorption shoulders at 550 and 600 nm. After treatment with a fluence of 60 J/cm^2, the P3HT:PCBM blend film has faded. The changes in the functional groups of a P3HT film after IPWL treatment were directly investigated using infrared spectroscopy (IR). After IPWL irradiation at a fluence of 60 J/cm^2, signals characteristic of carbonyl groups (C═O, 1731 cm^{-1}) and thiocarbonyl groups (C═S, 1107 cm^{-1}) appeared (see Supporting Information Figure S3), which means that P3HT undergoes degradation and oxidation during IPWL treatment with a strong fluence.[57,58]

We varied the pulse parameters to investigate the effects of pulse control on the IPWL treatment of the P3HT:PCBM blends. The pulse duration time was varied from 0.5 to 7 ms while maintaining a fixed total fluence to examine the effects of varying the irradiation time. For pulse duration times up to 1 ms, the photovoltaic performance increases. However, further increases in the pulse duration times above 1 ms reduce J_{sc} and PCE. This suggests that short pulses are preferred to prevent

degradation of the P3HT:PCBM blend films. We also varied the free temporal period from 5 to 40 ms while maintaining a fixed total fluence and pulse duration time to investigate the optimum time scale for self-organization of P3HT:PCBM blend films (see Supporting Information Figure S4). For a free temporal period up to 20 ms (total process time = 2.2 s), J_{sc} and PCE increase with increase of free temporal period; above 20 ms, the photovoltaic performance is saturated. This means that an IPWL treatment of 2.2 s is sufficient to induce the self-organization of the P3HT:PCBM blend film and to enhance the performance of the device.

Figure 5c shows the $J-V$ characteristics of PSCs constructed on a flexible substrate in either pristine condition or after IPWL treatment. The pristine device exhibits poor performance: J_{sc} = −3.19 mA/cm^2, V_{oc} = 0.71 V, FF = 0.36, and PCE = 0.81%. In contrast, the IPWL-treated device exhibits enhanced performance: J_{sc} = −6.86 mA/cm^2, V_{oc} = 0.57 V, FF = 0.53, and PCE = 2.06%; these values are comparable to those reported for a P3HT:PCBM solar cell based on a flexible substrate.[59] This demonstrates that the proposed IPWL treatment is substantially compatible with the R2R production of flexible PSCs.[34−36]

4. CONCLUSIONS

We have demonstrated that IPWL treatment can be used as an alternative to thermal treatments to control nanostructure of a BHJ-based photoactive layer. By performing IPWL treatment for 2.2 s on P3HT:PCBM blend films, the PCEs of the devices are improved to values close to those of devices after a typical thermal treatment. Pulsed-light irradiation with an optimized fluence can provide sufficient energy and temperature increase to induce the required phase transition in P3HT:PCBM blend films. Furthermore, we confirmed that the crystallinity and light-absorption properties of P3HT:PCBM blend films are effectively controlled by pulse management. We believe that this technique can offer a split-second, large area, and cost-effective optical method for the highly productive R2R manufacture of PSCs.

■ ASSOCIATED CONTENT

Ⓢ Supporting Information

AFM, photographs, and IR of pristine and IPWL-treated P3HT:PCBM blend films. Variation in the $J-V$ characteristics, J_{sc}, and PCE of IPWL-treated P3HT:PCBM blend films with the pulse duration time and free temporal period. Video of the IPWL process. This material is available free of charge via the Internet at http://pubs.acs.org.

■ AUTHOR INFORMATION

Corresponding Author

*E-mail: jalim@kist.re.kr; Tel. +82-2-958-5378.

Notes

The authors declare no competing financial interest.

■ ACKNOWLEDGMENTS

This work was supported by the Korea Institute of Science and Technology (KIST) Future Resource Research Program (2E24011) and Industrial Core Technology Development Program (2M30970) from the Ministry of Trade, Industry & Energy (MOTIE) and by the Basic Science Research Program through the National Research Foundation of Korea (NRF) funded by the Ministry of Education, Science and Technology (2011-0025491).

■ REFERENCES

(1) Brabec, C. J.; Dyakonov, V.; Parisi, J.; Sariciftci, N. S. *Organic Photovoltaics: Concepts and Realization*; Springer: New York, 2003; pp 159−248.
(2) Servaites, J. D.; Yeganeh, S.; Marks, T. J.; Ratner, M. A. *Adv. Funct. Mater.* **2010**, *20*, 97−104.
(3) Espinosa, N.; Hösel, M.; Angmo, D.; Krebs, F. C. *Energy Environ. Sci.* **2012**, *5*, 5117−5132.
(4) Darling, S. B.; You, F. *RSC Adv.* **2013**, *3*, 17633−17648.
(5) Hösel, M.; Søndergaard, R. R.; Jørgensen, M.; Krebs, F. C. *Energy Technol.* **2013**, *1*, 102−107.
(6) Krebs, F. C.; Hösel, M.; Corazza, M.; Roth, B.; Madsen, M. V.; Gevorgyan, S. A.; Søndergaard, R. R.; Karg, D.; Jørgensen, M. *Energy Technol.* **2013**, *1*, 378−381.
(7) Søndergaard, R. R.; Hösel, M.; Krebs, F. C. *J. Polym. Sci., Part B: Polym. Phys.* **2013**, *51*, 16−34.
(8) Yu, G.; Gao, J.; Hummelen, J. C.; Wudi, F.; Heeger, A. J. *Science* **1995**, *270*, 1789−1791.
(9) Barbec, C. J.; Winder, C.; Sariciftci, N. S.; Hummelen, J. C.; Dhanabalan, A.; van Hal, P. A.; Janssen, R. A. J. *Adv. Funct. Mater.* **2002**, *12*, 709−712.
(10) Kroeze, J. E.; Savenije, T. J.; Vermeulen, M. J. W.; Warman, J. M. *J. Phys. Chem. B* **2003**, *107*, 7696−7705.
(11) Theander, M.; Yartsev, A.; Zigmantas, D.; Sundström, V.; Mammo, W.; Andersson, M. R.; Inganäs, O. *Phys. Rev. B* **2000**, *61*, 12957−12963.
(12) Yang, Y.; Mielczarek, K.; Aryal, M.; Zakhidov, A.; Hu, W. *ACS Nano* **2012**, *6*, 2877−2892.
(13) Yang, H. Y.; Kang, N. S.; Hong, J.-M.; Song, Y.-W.; Kim, T. W.; Lim, J. A. *Org. Electron.* **2012**, *13*, 2688−2695.
(14) Riedel, I.; Dyakonov, V. *Phys. Status Solidi A* **2004**, *201*, 1332−1341.
(15) Li, G.; Shrotriya, V.; Huang, J.; Mariarty, T.; Emery, K.; Yang, Y. *Nat. Mater.* **2005**, *4*, 864−868.
(16) Irwin, M. D.; Buchholz, D. B.; Hains, A. W.; Chang, R. P. H.; Marks, T. J. *Proc. Natl. Acad. Sci. U.S.A.* **2008**, *105*, 2783−2787.
(17) Mihailetchi, V. D.; Xie, H.; de Boer, B.; Koster, L. J. A.; Blom, P. W. M. *Adv. Funct. Mater.* **2006**, *16*, 699−708.
(18) Zhao, Y.; Xie, Z. Y.; Qu, Y.; Geng, Y. H.; Wang, L. X. *Appl. Phys. Lett.* **2007**, *90*, 043504-1−043504-3.
(19) Huang, J.-H.; Li, K.-C.; Kekuda, D.; Padhy, H. H.; Lin, H.-C.; Hoc, K.-C.; Chu, C.-W. *J. Mater. Chem.* **2010**, *20*, 3295−3300.
(20) Kekuda, D.; Huang, J.-H.; Ho, K.-C.; Chu, C.-W. *J. Phys. Chem. C* **2010**, *114*, 2764−2768.
(21) Ko, C.-J.; Lin, Y.-K.; Chen, F.-C. *Adv. Mater.* **2007**, *19*, 3520−3523.
(22) Yoshikawa, O.; Sonobe, T.; Sagawa, T.; Yoshikawa, S. *Appl. Phys. Lett.* **2009**, *94*, 083301-1−083301-3.
(23) Flügge, H.; Schmidt, H.; Riedl, T.; Schmale, S.; Rabe, T.; Fahlbusch, J.; Danilov, M.; Spieker, H.; Schöbel, J.; Kowalsky, W. *Appl. Phys. Lett.* **2010**, *97*, 123306-1−123306-3.
(24) Okaraku, E. W.; Gupta, M. C.; Wright, K. D. *Sol. Energy Mater. Sol. Cells* **2010**, *94*, 2013−2017.
(25) Kim, H.-S.; Dhage, S. R.; Shim, D.-E.; Hahn, H. T. *Appl. Phys. A: Mater. Sci. Process.* **2009**, *97*, 791−798.
(26) Dhage, S. R.; Hahn, H. T. *J. Phys. Chem. Solids* **2010**, *71*, 1480−1483.
(27) Kang, J. S.; Ryu, J.; Kim, H. S.; Hahn, H. T. *J. Electron. Mater.* **2011**, *40*, 2268−2277.
(28) Lee, D. J.; Park, S. H.; Jang, S.; Kim, H. S.; Oh, J. H.; Song, Y. W. *J. Micromech. Microeng.* **2011**, *21*, 125023−1−7.
(29) Han, W.-S.; Hong, J.-M.; Kim, H.-S.; Song, Y.-W. *Nanotechnology* **2011**, *22*, 395705−1−6.
(30) Perelaer, J.; Abbel, R.; Wünscher, S.; Jani, R.; van Lammeren, T.; Schubert, U. S. *Adv. Mater.* **2012**, *24*, 2620−2625.
(31) Hösel, M.; Krebs, F. C. *J. Mater. Chem.* **2012**, *22*, 15683−15688.

(32) Angmo, D.; Larsen-Olsen, T. T.; Jørgensen, M.; Søndergaard, R. R.; Krebs, F. C. *Adv. Energy. Mater.* **2013**, *3*, 172−175.
(33) Ryu, J.; Kim, H.-S.; Hahn, H. T. *J. Electron. Mater.* **2011**, *40*, 42−50.
(34) Dhage, S. R.; Kim, H.-S.; Hahn, H. T. *J. Electron. Mater.* **2011**, *40*, 122−126.
(35) Song, Y.-W.; Park, S.-H.; Han, W.-S.; Hong, J.-M.; Kim, H.-S. *Mater. Lett.* **2011**, *65*, 2510−2513.
(36) Helgesen, M.; Carlé, J. E.; Andreasen, B.; Hösel, M.; Norrman, K.; Søndergaard, R.; Krebs, F. C. *Polym. Chem.* **2012**, *3*, 2649−2655.
(37) Huang, J.; Kaner, R. B. *Nat. Mater.* **2004**, *3*, 783−786.
(38) Krebs, F. C.; Norrman, K. *ACS Appl. Mater. Interfaces* **2010**, *2*, 877−887.
(39) Ajayan, P. M.; Terrones, M.; de la Guardia, A.; Huc, V.; Grobert, N.; Wei, B. Q.; Lezec, H.; Ramanath, G.; Ebbesen, T. W. *Science* **2002**, *296*, 705−705.
(40) Wang, N.; Yao, B. D.; Chan, Y. F.; Zhang, X. Y. *Nano Lett.* **2003**, *3*, 475−479.
(41) Cote, L. J.; C.-Silva, R.; Huang, J. *J. Am. Chem. Soc.* **2009**, *131*, 11027−11032.
(42) Zhao, J.; Swinnen, A.; Assche, G. V.; Manca, J.; Vanderzande, D.; Mele, B. V. *J. Phys. Chem. B* **2009**, *113*, 1587−1591.
(43) De Albuquerque, J. E.; Melo, W. L. B.; Fria, R. M. *Rev. Sci. Instrum.* **2003**, *74*, 306−308.
(44) De Albuquerque, J. E.; Melo, W. L. B.; Fria, R. M. *J. Polym. Sci., Part B* **2000**, *38*, 1294−1300.
(45) Malik, S.; Nandi, A. K. *J. Polym. Sci., Part B: Polym. Phys.* **2002**, *40*, 2073−2085.
(46) Yamamoto, T. *J. Chem. Phys.* **1997**, *107*, 2653−2663.
(47) Yamamoto, T. *Polymer* **2004**, *45*, 1357−1364.
(48) Sasaki, T.; Ikeda, T.; Ichimura, K. *Macromolecules* **1992**, *25*, 3807−3811.
(49) Chen, D.; Liu, F.; Wang, C.; Nakahara, A.; Russell, T. P. *Nano Lett.* **2011**, *11*, 2071−2078.
(50) Li, G.; Shrotriya, V.; Yao, Y.; Yang, Y. *J. Appl. Phys.* **2005**, *98*, 043704−1−3.
(51) Huang, Y.-C.; Liao, Y.-C.; Li, S.-S.; Wu, M.-C.; Chen, C.-W.; Su, W.-F. *Sol. Energy Mater. Sol. Cells* **2009**, *93*, 888−892.
(52) Yang, X.; Loos, J.; Veenstra, S. C.; Verhees, W. J. H.; Wienk, M. M.; Kroon, J. M.; Michels, M. A. J.; Janssen, R. A. J. *Nano Lett.* **2005**, *5*, 579−583.
(53) van Bavel, S.; Sourty, E.; de With, G.; Frolic, K.; Loos, J. *Macromolecules* **2009**, *42*, 7396−7403.
(54) Gadisa, A.; Svensson, M.; Andersson, M. R.; Inganäs, O. *Appl. Phys .Lett.* **2004**, *84*, 1609−1611.
(55) Hintz, H.; Peisert, H.; Egelhaaf, H.-J.; Chassé, T. *J. Phys. Chem. C* **2011**, *115*, 13373−13376.
(56) Manceau, M.; Rivaton, A.; Gardette, J.-L.; Guillerez, S.; Lemaître, N. *Polym. Degrad. Stab.* **2009**, *94*, 898−907.
(57) Matturro, M. G.; Reynolds, R. P.; Kastrup, R. V.; Pictroski, C. F. *J. Am. Chem. Soc.* **1986**, *108*, 2775−2776.
(58) Abdou, M. S. A.; Holdcroft, S. *Macromolecules* **1993**, *26*, 2954−2962.
(59) Na, S.-I.; Kim, S.-S.; Jo, J.; Kim, D.-Y. *Adv. Mater.* **2008**, *20*, 4061−4067.